Applied Scientific Research **53:** 321–338, 1994.

The Proper Orthogonal Decomposition, Wavelets and Modal Approaches to the Dynamics of Coherent Structures *

GAL BERKOOZ, JUAN ELEZGARAY, PHILIP HOLMES,
JOHN LUMLEY** and ANDREW POJE
Cornell University, Sibley School of Mechanical and Aerospace Engineering, Ithaca, NY 14853-7501, U.S.A.

Received 8 September 1993; accepted in revised form 19 April 1994

Abstract. We present brief précis of three related investigations. Fuller accounts can be found elsewhere. The investigations bear on the identification and prediction of coherent structures in turbulent shear flows. A second unifying thread is the Proper Orthogonal Decomposition (POD), or Karhunen–Loève expansion, which appears in all three investigations described. The first investigation demonstrates a close connection between the coherent structures obtained using linear stochastic estimation, and those obtained from the POD. Linear stochastic estimation is often used for the identification of coherent structures. The second investigation explores the use (in homogeneous directions) of wavelets instead of Fourier modes, in the construction of dynamical models; the particular problem considered here is the Kuramoto–Sivashinsky equation. The POD eigenfunctions, of course, reduce to Fourier modes in homogeneous situations, and either can be shown to converge optimally fast; we address the question of how rapidly (by comparison) a wavelet representation converges, and how the wavelet-wavelet interactions can be handled to construct a simple model. The third investigation deals with the prediction of POD eigenfunctions in a turbulent shear flow. We show that energy-method stability theory, combined with an anisotropic eddy viscosity, and erosion of the mean velocity profile by the growing eigenfunctions, produces eigenfunctions very close to those of the POD, and the same eigenvalue spectrum at low wavenumbers.

1. Introduction

Coherent structures are observed in most turbulent flows. Their relative intensity depends on inflow and boundary conditions, flow geometry and streamwise position in the flow. It is tempting to think that they may represent instability modes either of a laminar precursor or of the turbulent flow, which have grown to non-linear maturity. Dynamical models can be constructed using these coherent structures, which can then be used for many purposes: prediction of transport or noise, active control of the flow, and so forth. Such possibilities raise several questions: how best to identify structures in experimental data; how to predict structures in flows

* Prepared for presentation at International Union of Theoretical and Applied Mechanics Symposium "Eddy Structure Identification in Free Turbulent Shear Flows", Poitiers, France, 12–14 October 1992. Supported in part by: the U.S. Air Force Office of Scientific Research, The U.S. Office of Naval Research (Mechanics Branch and Physical Oceanography Program), and the U.S. National Science Foundation (program in Physical Oceanography).
** Author for correspondence.

that have not been extensively documented; what mathematical choices to make in implementing such models.

The Proper Orthogonal Decomposition or Karhunen–Loève expansion has been used for the identification of coherent structures (Aubry et al., 1988). It has been shown in many respects to be optimum. However, other techniques have also been put forward, in particular linear stochastic estimation (Adrian, 1979). We would like to know what connections there may be between these two methods for identifying coherent structures. Below (in Section 2) we explore this.

Many flows are homogeneous in one or more directions. In a homogeneous direction, the POD reduces to a Fourier representation. Such a representation is optimum, in the sense that it converges no slower, and usually faster, than any other representation. However, a Fourier representation is not particularly well suited to phenomena in a turbulent flow. Fourier modes are of infinite spatial extent, while eddies in a turbulent flow are quite finite in their spatial extent. A much more attractive possibility would be the wavelet, since it also is of limited extent, but this is not optimum. Just how far from optimum is it? If we use wavelets, we will have wavelet-wavelet interactions in space, and we have to make a decision regarding appropriate truncations of these interactions. In Section 3 we examine these questions.

Obtaining the POD eigenfunctions for a given flow either requires extensive experimental measurements (Herzog, 1986), or extensive post-processing of data from direct numerical simulation of the flow. Either is expensive and time-consuming. We would like a simpler way of obtaining the eigenfunctions, particularly in flows for which neither DNS nor extensive measurement exist. In particular, we can implement our suspicion that the coherent structures may (at least in some circumstances) result from a disturbance of the turbulent profiles of mean velocity and stress, a disturbance which is unstable, and which grows non-linearly, leading the system to a new attractor, consisting of the flow plus coherent structures (Poje and Lumley, 1991; Leibovich, 1991). In this new stable state, we may hope that the coherent structures will resemble the non-linear growth phase of the instability mode. We pursue these questions in Section 4 below.

2. Linear Stochastic Estimation

In this section we comment on the connection between the POD and linear stochastic estimation, as applied by Adrian and coworkers in Adrian (1979), Adrian and Moin (1988), Adrian, Moin and Moser (1987) and Moin, Adrian and Kim (1987). Elaboration of this material can be found in Berkooz (1991). Suppose one wanted to find an estimate for $u(x)$ given $u(x')$ (at some other point), an estimate which would minimize the mean square difference between $u(x)$ and the estimate. For the sake of simplicity of exposition, we limit ourselves to complex scalar functions of a single variable. Suppose, moreover, that one seeks an estimate linear in $u(x')$; this is called a linear stochastic estimate. We are examining $V(x, x')$ such that

$V(x,x')u(x')$ will be the estimate for $u(x)$, and we want to search through the class $V(x,x')$ to find $A(x,x')$ such that:

$$\min_{V(x,x')} \langle |u(x) - V(x,x')u(x')|^2 \rangle = \langle |u(x) - A(x,x')u(x')|^2 \rangle \tag{1}$$

is achieved by $A(x,x')$. We indicate by $\langle \cdot \rangle$ an ensemble average. We use the classical calculus of variations (cf. Adrian, 1979), which leads directly to:

$$A(x,x') = \langle u(x)u^*(x') \rangle \cdot \langle u(x')u^*(x') \rangle^{-1}. \tag{2}$$

In (2) the two point correlation tensor $R(x,x') = \langle u(x)u^*(x') \rangle$ appears with a normalization. Using classical results for the POD, we can write (Berkooz, 1991)

$$A(x,x') = \frac{\sum_{i=1}^{\infty} \lambda_i \phi_i(x)\phi_i^*(x')}{\sum_{i=1}^{\infty} \lambda_i |\phi_i(x')|^2} = \sum_{i=1}^{\infty} \phi_i(x) f_i(x'), \tag{3}$$

where $f_i(x') = \lambda_i \phi_i^*(x') / \sum_{j=1}^{\infty} \lambda_j |\phi_j(x')|^2$. We may interpret $f_i(x')$ as the relative contribution of ϕ_i to $u(x')$ on the average.

It is remarkable, and is the point of this section, that we get exactly the same result from a simplified PDF model based on the POD. Here we assume that the coefficients a_i in a modal expansion $u(x,t) = \Sigma a_i(t)\phi_i(x)$ are jointly normal and independent, with zero mean and variance λ_i. Let us compute the estimator $\langle u(x) \mid u(x') \rangle$. Since we have an expression for the PDF (through our assumption on the a_i) we can compute this explicitly. Recall from probability theory that if the x_i are independent and normal with zero mean and variance σ_i^2 for $i = 1, \ldots, m$ then

$$\left\langle x_i \mid \sum_{j=1}^{m} x_j = C \right\rangle \frac{\sigma_i^2 C}{\sum_{j=1}^{m} \sigma_j^2}. \tag{4}$$

(See the formula for the conditional expectation of joint normal variables in Feller, 1957.) Using (4), we have

$$\left\langle a_i\phi_i(x') \mid \sum_{j=1}^{\infty} a_j\phi_j(x') = u(x') \right\rangle = \frac{\lambda_i |\phi_i(x')|^2 u(x')}{\sum_{j=1}^{\infty} \lambda_j |\phi_j(x')|^2} \tag{5}$$

which gives (Berkooz, 1991)

$$\begin{aligned} \langle u(x) \mid u(x') \rangle &= \frac{\sum_{i=1}^{\infty} \lambda_i |\phi_i(x')|^2 u(x')\phi_i(x)/\phi_i(x')}{\sum_{j=1}^{\infty} \lambda_j |\phi_i(x')|^2} \\ &= \frac{\sum_{i=1}^{\infty} \lambda_i \phi_i^*(x')\phi_i(x)u(x')}{\sum_{j=1}^{\infty} \lambda_j |\phi_j(x')|^2}. \end{aligned} \tag{6}$$

This is exactly the same result obtained from linear stochastic estimation: (3).

This single result helps to place linear stochastic estimation in context: it is not a different animal altogether, but is just the POD with a simplifying assumption on the PDF of the coefficients. As long as we are not discussing transport (which probably requires non-zero third moments) the assumption on the coefficients is physically not unrealistic.

3. Wavelets

All the flows of interest to us have one or more homogeneous directions. We are accustomed to use in these directions the Fourier transform, which is the homogeneous equivalent of the POD. However, the Fourier transform is not nearly so appropriate in the homogeneous case as is the POD in the inhomogeneous case. This is because the Fourier modes are not confined to a neighborhood, but extend to infinity without attenuation. All disturbances in fluid, and coherent structures in particular, are localized. There is therefore considerable motivation to find another representation that is more appropriate.

In Tennekes and Lumley (1972) it was suggested that a more appropriate quantity would be the energy surrounding a wavenumber κ, say from κ/a to $a\kappa$, where $a = 1.62$. In physical space, this packet with appropriate phase relations is confined to a region, essentially dropping to zero in about $2\pi/\kappa$ from the origin. Tennekes and Lumley called these 'eddies', but the are an example of what are now called wavelets.

While wavelets appear to make more physical sense, we might worry because we would be discarding the optimality of the Fourier representation; would convergence be much slower, so that we would need many more terms, or would we lose considerable energy if we used the same number of terms? A main result of a recent paper (Berkooz et al., 1992) is that very little energy is lost when using a wavelet basis instead of a Fourier basis. Although wavelets are physically appealing, it would also be nice to have reassurance from calculations that physical behavior would be preserved in a wavelet representation in which interactions are truncated. To set our minds at rest on this point, Berkooz et al. (1992) also display a *relatively* low-dimensional wavelet model of the Kuramoto–Sivashinsky equation with truncated interactions that shows dynamical behavior similar to the full equation.

Without getting involved with mathematical details, an orthonormal wavelet basis is constructed by starting with a function, say $\Psi(x)$, similar to the eddy suggested by Tennekes and Lumley (1972). From this, construct a set $\Psi_{j,0}(x) = \Psi(x2^j)$, $j = 1, 2, \ldots$ Each of these is shrunk affinely, but is geometrically similar to the original function. Now consider the translates of $\Psi_{j,0}$: $\Psi_{j,k}(x) = \Psi_{j,0}(x - k2^j)$, $k = 1, 2, \ldots$

Berkooz et al. (1992) consider a periodic, homogeneous stochastic process. It is then obvious that the POD decomposition becomes identical to the Fourier decomposition. Now, if, for a given ε, we need $N(\varepsilon)$ POD modes in order to satisfy

$$\left| \sum_{i \leq 1} \langle a_i(t)|^2 \rangle - \sum_{i=1}^{N(\varepsilon)} \langle |a_i(t)|^2 \rangle \right| \leq \varepsilon \tag{7}$$

then, if the $\{b_i\}$ are the coefficients in a wavelet basis, they show that, for some constant C, depending only on the process (and not on ε):

$$\Big| \sum_{i\geq 1} \langle |a_i(t)|^2 \rangle - \sum_{i=1}^{\mathcal{N}(\varepsilon)} |b_i(t)|^2 \rangle \Big| \leq C\varepsilon \tag{8}$$

for some $\mathcal{N}(\varepsilon) > N(\varepsilon)$ only slightly bigger than $N(\varepsilon)$ (the precise statement is given in Berkooz et al., 1992). This suggests that we will not be too much worse off using a wavelet basis, but it would be reassuring to have numerical confirmation.

3.1. NUMERICAL RESULTS

Berkooz et al. (1992) wished to apply these ideas to a simple situation. The three-dimensional, three component Navier–Stokes equations are too complicated for a first effort.

The one-dimensional, scalar Kuramoto–Sivashinsky (K–S) equation appears in a variety of contexts, such as quasi-planar fronts, chemical turbulence, etc. It shares some properties with Burgers' equation and the Navier–Stokes equations, but is much easier to deal with. Up to a rescaling, this equation can be written as:

$$u_t + u_{xx} + u_{xxxx} + u_x u = 0, \quad 0 \leq x \leq L \tag{9}$$

u periodic on $[0, L]$, where L, the length of the spatial domain, is the only free parameter in the problem.

Although the dynamical behavior for small values of L is fairly well understood (see Hymans and Nicolaenko, 1986 for an overview), many open questions remain concerning the limit $L \to \infty$ (Zaleski, 1989; Pomeau et al., 1984). As can be seen from the numerical simulations, for $L > 30$, a chaotic regime involving both space and time disorder occurs (see Fig. 1, where we plot a space-time representation of a typical solution, $L = 400$, $0 \leq t \leq 100$; the grey scale represents the magnitude of u).

In order to check the estimate (8), we compare the energy resolved by a given number of modes using either a Fourier (POD) or wavelet basis. Note that, to compare the Fourier and wavelet bases, all the translates in the wavelet basis must be considered. Here are some results (see Fig. 2; the numbers indicate the percentage of the mean of u^2 that is captured by the indicated number of modes):

Number of modes	wavelets ($m = 6$)	wavelets ($m = 8$)	Fourier
64 ($j = 6$)	70.84%	71.5%	72.2%
96 ($j = 6, 5$)	79.1%	79.43%	83.3%
127 ($0 \leq j \leq 6$)	84.1%	84.9%	89.7%
255 ($0 \leq j \leq 7$)	99.9%	99.9%	99.9%

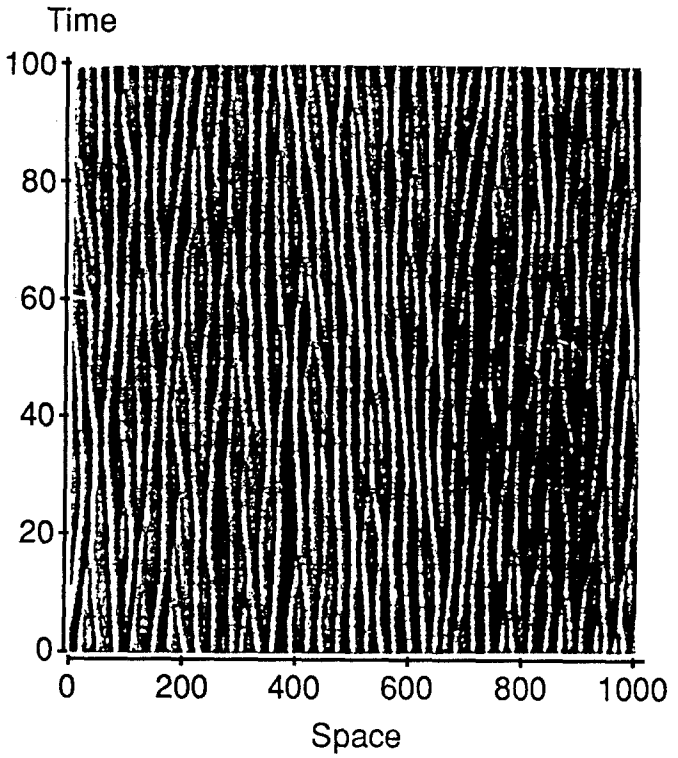

Fig. 1. A typical solution of the periodic Kuramoto–Sivashinsky equation ($L = 400$).

The scale $j = 6$ which captures most of the energy on the average, corresponds to a characteristic length $2^{-6}L \approx q_m^{-1}$, which is also the length scale associated with the most unstable wavelength q_m. In agreement with the general shape of the energy spectrum, the scales $0 \leq j \leq 5$ are shown to capture more energy than the scales in the dissipative range ($j \geq 7$). The above figures show that (for sufficiently smooth splines) the wavelet projection captures almost the same amount of energy as the Fourier (= POD) decomposition (within 5%).

These results prompted Berkooz et al. (1992) to conclude that from an average energy point of view wavelets were a reasonable candidate for a modal decomposition of the K–S equation. The localized nature of the wavelets may give a unique view of the spatial attributes of the coherent structures. We outline their approach. They conjecture the existence of a dynamically relevant length scale L_C such that interactions between physical regions of distance greater than L_C are dynamically insignificant (a dynamical St. Venant principle). Determining the validity of this conjecture is part of their study. They use this conjecture to remove terms in a wavelet-Galerkin projection that correspond to interactions between regions of distance greater than L_C. To study whether the dynamics of coherent structures are indeed locally determined they construct truncations corresponding to a small box size L_B in the larger box of size L.

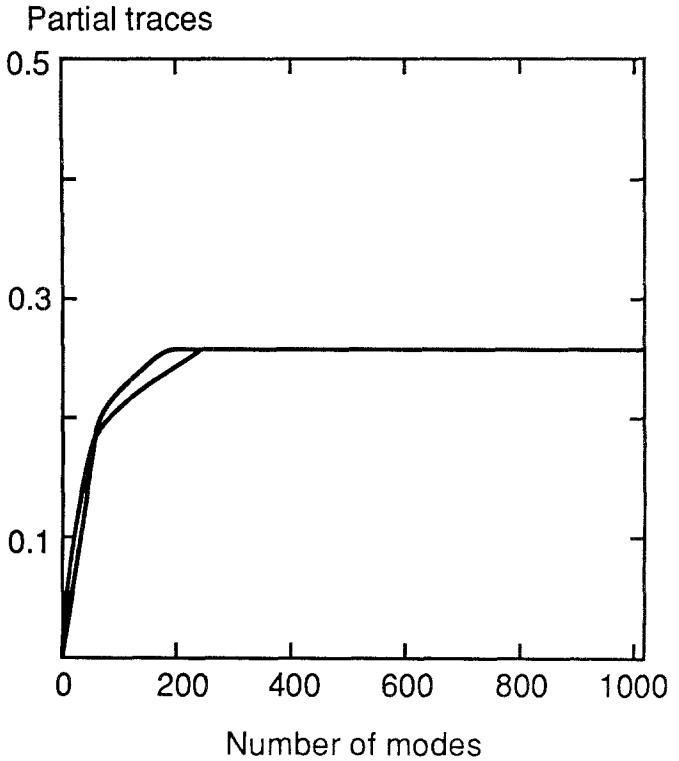

Fig. 2. The energy resolved by the Fourier (POD) basis (upper curve) and the wavelet basis (lower curve), as functions of the number of modes.

They need to address the role of unresolved physical space (i.e. modes located outside the box of size L_B). It is obvious that the Dirichlet type of boundary condition imposed will create a boundary layer which will affect the dynamics, especially in small boxes which are of interest to us. There are two plausible approaches to remove this effect. One approach uses a stochastic boundary condition (which is hard to implement numerically and treat analytically). The other approach appeals to the conjecture on the existence of L_C. One takes a box of size L_B greater than $2L_C$ so that one can periodize the small model using resolved relatively distant modes instead of unresolved ones. They opted for the second approach.

We present some preliminary results of the integration of one such model. They resolved a box of size $L_B = 50$ (this is 1/8 of the original box). Figure 3 shows the spatio-temporal evolution of the full system, with a Fourier basis. Figure 4 shows the spatio-temporal evolution of a (rescaled) model with $L_C = 50 \times 3/8$, which is in excellent qualitative agreement with the dynamics of the full system. As in Fig. 1, Figs 3 and 4 indicate by grey scale the magnitude of u. If L_C is too small, after a long initial transient, the system eventually settles down to a periodic oscillatory state, in which no interaction between the localized structures is observed. This can be avoided by an increase in L_C, which adds significant non-linear interactions

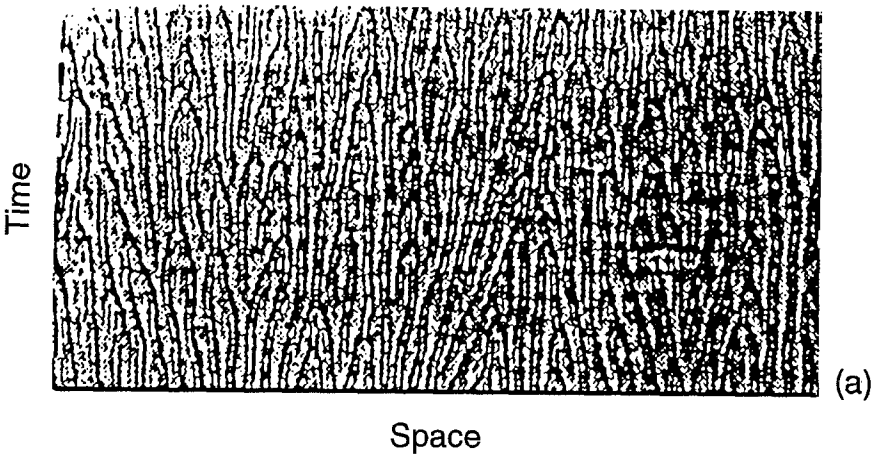

Fig. 3. Full simulation of the Kuramoto–Sivashinsky equation (Fourier basis).

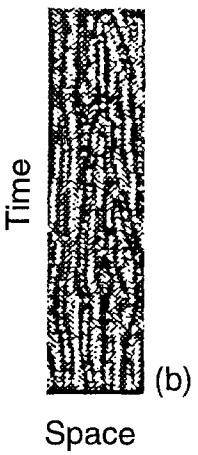

Fig. 4. Wavelet simulation of the K–S equation (4 mode) with $L_B = 50$ (rescaled).

between relatively distant physical space locations. It might also be avoided by a stochastic boundary condition.

Thus we see that: we do not lose any significant amount of energy by changing from a Fourier to a wavelet basis; and it is possible to use a wavelet basis with truncated spatial interaction to reproduce complex dynamical behavior reminiscent of that governed by the Navier–Stokes equations.

4. Eduction of Coherent Structures

Ideally, one would like to apply the POD approach to a wide range of flows where coherent structures are known to play an important role in the dynamics. The POD procedure, however, requires the two-point velocity autocorrelation tensor as

input, thus necessitating complete documentation of the flow before the analysis can proceed. For flows with very high Reynolds numbers or complicated geometries this can be prohibitively expensive given current computational and experimental capabilities. In this section we will describe an analytic procedure for extracting basis functions (structures) which approximate those given by the POD but which requires much less *a priori* statistical information about the flow.

The method presented here is based on energy stability considerations put forth by Lumley (1971). A fuller description can be found in Poje (1993); Poje and Lumley (1994). First, the instantaneous flow field is decomposed into three components in order to isolate the large scale structures. Evolution equations can then be written for the coherent velocity field and the coherent kinetic energy. A procedure can then be formalized to search for the structures which maximize the instantaneous growth rate of coherent energy, the rationale being that the structures which on average have the largest growth rates will compare well with the structures which contribute the most to the average turbulent kinetic energy (POD eigenfunctions).

As an example we consider turbulent channel flow assumed statistically homogeneous in both the downstream (x_1) and cross-stream (x_3) directions. In order to extract spatial structures from the total velocity field, we avoid traditional Reynolds averaging and instead decompose the instantaneous velocity field into three components: the spatial mean (U), the coherent field ($\mathbf{v}$) and the incoherent background turbulence ($\mathbf{u}'$).

$$u_i(\mathbf{x}, t) = U(x_2) + v_i(\mathbf{x}, t) + u_i'(\mathbf{x}, t). \tag{10}$$

The spatial mean is an average over the x_1–x_3 plane; we will indicate it by $[\ldots]$. We introduce a second averaging procedure, denoted by $\langle\ldots\rangle$, which eliminates the small-scale turbulence while leaving the coherent field intact.

$$\langle u_i(\mathbf{x}, t)\rangle = U(x_2) + v_i(\mathbf{x}, t). \tag{11}$$

Practically this can be accomplished in several ways (Reynolds and Hussain, 1972; Liu, 1988; Brereton and Kodal, 1992; Berkooz, 1991). We will refer to this average as a phase average. For our purpose here it is sufficient that the phase average and space average commute, and that the cross-correlations be negligible.

$$\langle u_i' v_j\rangle = [u_i' v_j] = 0. \tag{12}$$

It is possible to devise various models to support Equation (12). Given these averaging procedures, we can manipulate the Navier–Stokes equations to arrive at evolution equations for the coherent velocity field.

$$Dv_i/Dt + v_j v_{i,j} = -\pi_{,i} + \nu v_{i,jj} + \tau_{ij,j} - S_{ij} v_j + [v_i v_j]_j \tag{13}$$

where D/Dt denotes the mean convective derivative, S_{ij} the mean rate of strain, and ν the kinematic viscosity, τ_{ij} represents the rectified effects of the small scale fluctuations on the coherent field and is defined by

$$\tau_{ij} = [u_i' u_j'] - \langle u_i' u_j'\rangle. \tag{14}$$

This can be thought of as a perturbed Reynolds stress, which is unknown and will ultimately require modeling. In the limit of a complete random turbulence containing no structure (i.e. $\langle \ldots \rangle = 0$) this quantity is equal to the usual Reynolds stress. In the case when the turbulence is completely structured so that $\langle \ldots \rangle = [\ldots]$, τ_{ij} is identically zero.

We now follow classical energy method stability analysis for the coherent field. First, the growth rate of the volume averaged coherent energy E is defined as a functional of the coherent velocity field.

$$\lambda(\mathbf{v}, U, \nu, \tau) = (1/2E)\, \mathrm{d}E/\mathrm{d}t. \tag{15}$$

Integration by parts and continuity are used to eliminate the non-linear convective and pressure terms. We seek the solenoidal velocity field which maximizes λ. Application of the calculus of variations then gives the Euler equations for the maximizing $\mathbf{v}$ field in the form of an eigenvalue relation.

$$\begin{aligned} &\lambda v_i + S_{ij} v_j = -\pi_{,i} + \nu v_{i,jj} + \tau_{ij,j} \\ &v_{i,i} = 0. \end{aligned} \tag{16}$$

We consider coherent fields which are periodic in the homogeneous directions. This allows a decomposition into poloidal and toroidal components which satisfy continuity exactly (Joseph, 1973)

$$v_1 = \Psi_{,12} - v_{,3}; \quad v_2 = -(\Psi_{,11} + \Psi_{,33}); \quad v_3 = \Psi_{,23} + v_{,1}. \tag{17}$$

The two scalar functions are then expanded in normal modes in the streamwise and spanwise directions.

$$\begin{aligned} \Psi(\mathbf{x}) &= \Psi(x_2) \exp\{i(k_1 x_1 + k_3 x_3)\} \\ v(\mathbf{x}) &= v(x_2) \exp\{i(k_1 x_1 + k_3 x_3)\}. \end{aligned} \tag{18}$$

Substituting the above into Equation (16) and eliminating the pressure π results in two coupled equations, forming a differential eigenvalue problem.

In order to proceed we need to specify a mean velocity field and a model for the unknown stress terms.

4.1. CLOSURE MODELS

We have investigated two different models for the unknown stress terms appearing in the eigenvalue relation. It should be noted that, modulo the modeled terms, Equation (16) is linear in the coherent velocities, providing an inexpensive means of determining basis functions. This linearity is an essential advantage of the method and for this reason we will constrain any stress model to be both linear and homogeneous in the $\mathbf{v}$ field insuring that the governing equation remains a regular eigenvalue problem. Tensorially this requires

$$\tau_{ij} - \tau_{kk}\delta_{ij}/3 = \Gamma_{ijkl}(v_{k,l} + v_{l,k}). \tag{19}$$

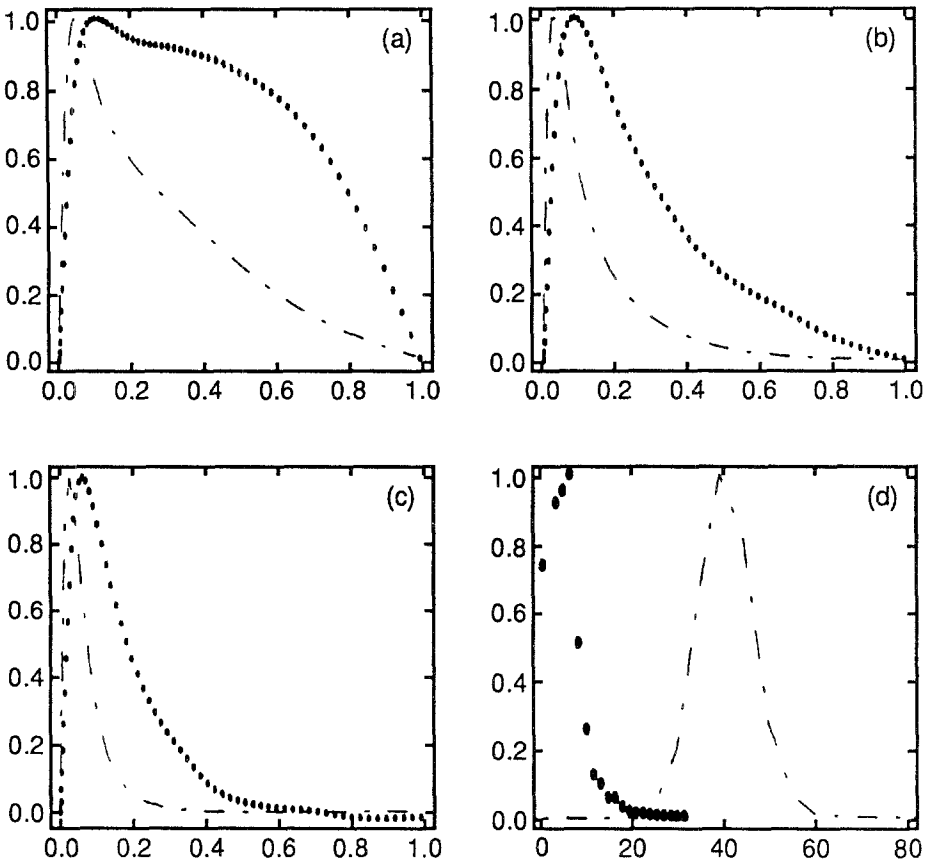

Fig. 5. Isotropic eddy viscosity model. •••• POD; ——·——·—— isotropic model; (a) $k_3 = 3.00$, (b) $k_3 = 6.00$, (c) $k_3 = 12.00$, (d) spectrum.

The nature of the averaging procedure implies that the scales of the coherent field and the background turbulence are different. Assuming that the background turbulence evolves on much shorter time and length scales than the structures, it seems plausible that a Newtonian stress-strain relationship like that for the molecular stresses will provide the basis for a model. We set

$$\tau_{ij} - \tau_{kk}\delta_{ij}/3 = \nu_t(v_{i,j} + v_{j,i}). \tag{20}$$

Due to the inhomogeneity of the turbulence in the wall normal direction, we specify ν_t as a function of x_2 corresponding to experimentally determined values of the traditional eddy viscosity. We will refer to this basic model as the isotropic eddy viscosity model.

Using the basic stress model and an analytic expression for the fully turbulent mean profile (Reynolds and Tiederman, 1967) we have solved the resulting equations numerically. Figure 5 shows comparisons between the calculated first order eigenvectors and the POD results of Moin and Moser (1989) obtained from a

numerical data base; the results are shown as a function of distance from the wall, for three different values of the cross-stream wavenumbers (recall that the streamwise wavenumber is zero). Figure 5d compares the first order eigenvalue spectrum obtained both ways, as a function of cross-stream wavenumber. Although there are qualitatively similarities in the shape of the structures, the modes predicted by the stability method fall off much more rapidly away from the wall than do the POD functions. The eigenvalue spectrum clearly shows that the stability analysis favors modes which have a much higher wavelength than the maximum energy modes of the POD.

Although there may be a number of reasons for this discrepancy, we choose to first examine more closely the closure model. We find that the isotropic eddy viscosity model creates no coupling between the different components of the coherent velocity. When there is no streamwise variation of the coherent field the only coupling terms in the equations are those multiplying the mean gradient. For realistic mean profiles, regions of high shear are confined to thin regions near the wall, and the structures predicted may be expected to fall off as quickly as the shear.

We now seek to develop a stress model that allows for some anisotropy in the eddy viscosity, and thus couples the component equations through the stress terms. We begin with the evolution equation for the Reynolds stresses, where we are obliged to model a number of terms to obtain a closed system. We use standard second-order turbulence models. We model the pressure-strain correlation by a return-to-isotropy term and an isotropization-of-production term (Naot et al., 1970); we use an isotropic dissipation. We assume the stresses are in local equilibrium: $D[u_i u_j]/Dt = 0$. This reduces the evolution equation for the Reynolds stress to an algebraic expression.

Now we set up a perturbation expansion in terms of mean field quantities, taking the coherent field as an order ε perturbation to the spatial mean. On physical grounds, we argue that the perturbed stress field is due entirely to the presence of the structures and consequently we restrict the model to include only production due directly to coherent velocity gradients. This is in agreement with a cascade analogy for the complete flow: the coherent structures are fed energy directly by the mean gradients while the small scale turbulence is in turn fed by gradients of the coherent field. If we identify the 0th order stresses with an eddy viscosity tensor, then the closure model can be written as

$$\tau_{ij} - \tau_{kk}\delta_{ij}/3 = -\nu_{ik}s_{kj} \tag{21}$$

where the tensor viscosity has the following structure in this specific case: $\nu_{13} = \nu_{23} = 0$, $\nu_{33} = \nu_{22}$.

Despite the absence of mean production terms, this model is still a major improvement over the isotropic eddy viscosity formulation. In the simple model the effects of the mean field have been neglected entirely. Here we have allowed for modulation of the perturbation stresses by the mean field through the 0th order stresses appearing in the production terms. Also we have unconstrained the model

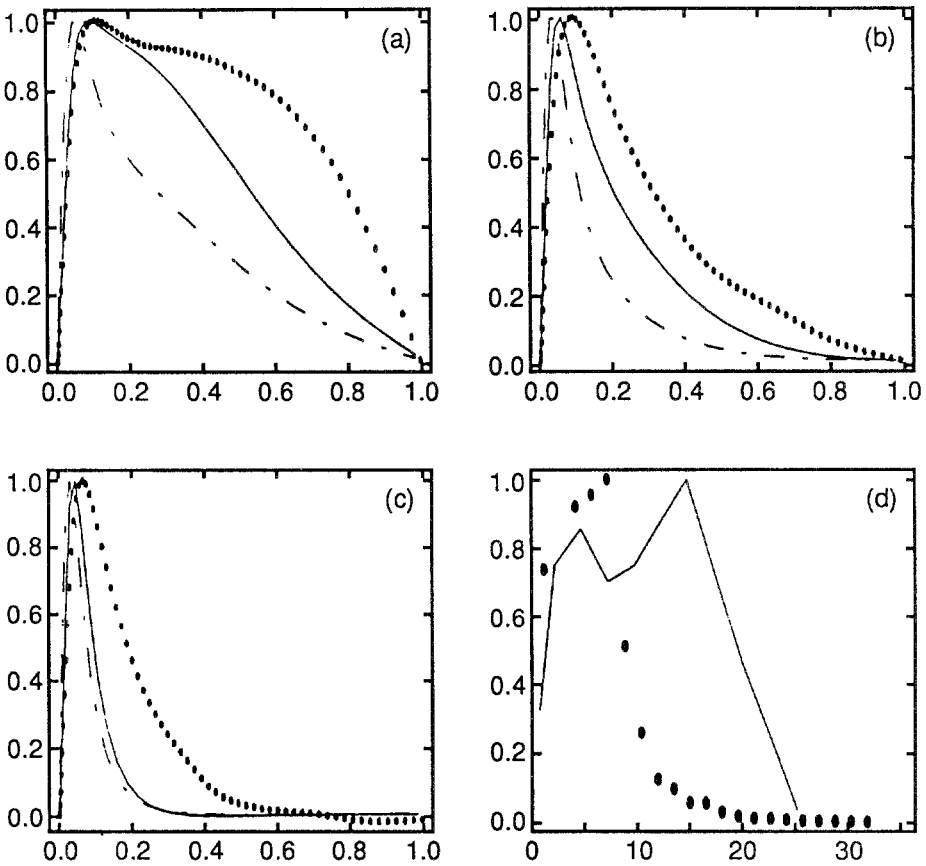

Fig. 6. Anisotropic eddy viscosity model: •••• POD; —·—·—·— isotropic model; —— anisotropic model; (a) $k_3 = 3.00$, (b) $k_3 = 6.00$, (c) $k_3 = 12.00$, (d) spectrum.

in an important way since the tensorial form of the eddy viscosity allows the principal axes of the stress tensor to be unaligned with the axes of the rate of strain. This is more realistic considering the three-dimensionality of the coherent field. This model leads to the expected cross-coupling of the equations through the stress terms.

Figure 6 shows eigensolutions for several values of k_3 (see the description of Fig. 5 for clarification). The results compare well with the POD eigenvalues, especially for wavenumbers at or below the peak in the POD spectrum. The improvement with decreasing wavenumber is expected given the modeling considerations. The separation of scales between the background turbulence and the coherent structures increases as the wavenumber decreases adding to the expected accuracy of the stress model. The comparison of the two models indicates significant improvements in the results given by the anisotropic eddy viscosity form. The energy method procedure with the more refined closure model appears capable of

extracting structures which closely approximate those given by the POD at least at the energy containing scales of motion.

Despite the general improvement, it is still clear that more needs to be done. From Figs 5 and 6, it is evident that the eigenspectrum produced by solution of Equation (10), while improved by the use of the anisotropic closure model, still predicts structures with maximum growth rate that are a factor of 2 smaller than those containing the most energy (as given by the POD). We next consider the effect on the spatial mean velocity field of the growing coherent perturbation.

4.2. INTERACTION WITH THE MEAN

At this point we consider the role of the mean velocity in the two methods. The POD structures are derived from solutions to the non-linear Navier–Stokes equations which allow for complicated interaction between the different scales of motion. The structures evolve in a mean velocity field that is changing due to the presence of the structures themselves. Conditionally averaged mean profiles clearly show the evolution of the local shear in the presence of coherent structures (see Fig. 7). It is clear from Fig. 8 that profiles with a larger region of high shear also have eigenfunctions which are non-negligible in a broader region. We see that structures, in the relatively long period before bursting, act to erode the shear that they see. The POD eigenfunctions are given by averages of contributions from different mean profiles.

The stability method on the other hand does not allow for any interaction between the mean and the coherent field. The mean flow is imposed and the resulting structures are calculated. The mean profiles we have used are time averages which mask any contribution from the coherent field. As such the stability analysis predicts that the highest growth modes are those which can best extract energy from the time averaged mean shear which is concentrated in the small near-wall region. Since the structures have an aspect ratio of about 1, the narrow region of high imposed shear leads to a peak in the eigenspectrum at a large wavenumber.

To allow the mean field to evolve under the influence of the coherent field, we follow Liu (1988) and write time evolution equations for the energy density of the coherent field. We allow the mean profile to depend on the coherent velocity as it does in reality. We expect that equilibrium solutions for the energy density as a function of cross-stream wavenumber will approximate the average energy content as given by the POD spectrum.

We assume that the coherent field is given by the eigenmodes of the stability problem, but we now allow them to vary in time

$$v_i(\mathbf{x}, t) = A(t)\Psi_i(\mathbf{x}) \tag{22}$$

$$\langle u_i u_j \rangle(\mathbf{x}, t) = E(t)B_{ij}(\mathbf{x}) \tag{23}$$

where $\Psi_1 = v\exp\{ikx_3\}$, $\Psi_2 = ik\Psi\exp\{ikx_3\}$, $\Psi_3 = -D\Psi\exp\{ikx_3\}$. By examining the evolution equation for $r_{ij} = \langle u_i u_j \rangle - [u_i u_j]$, the forcing terms are

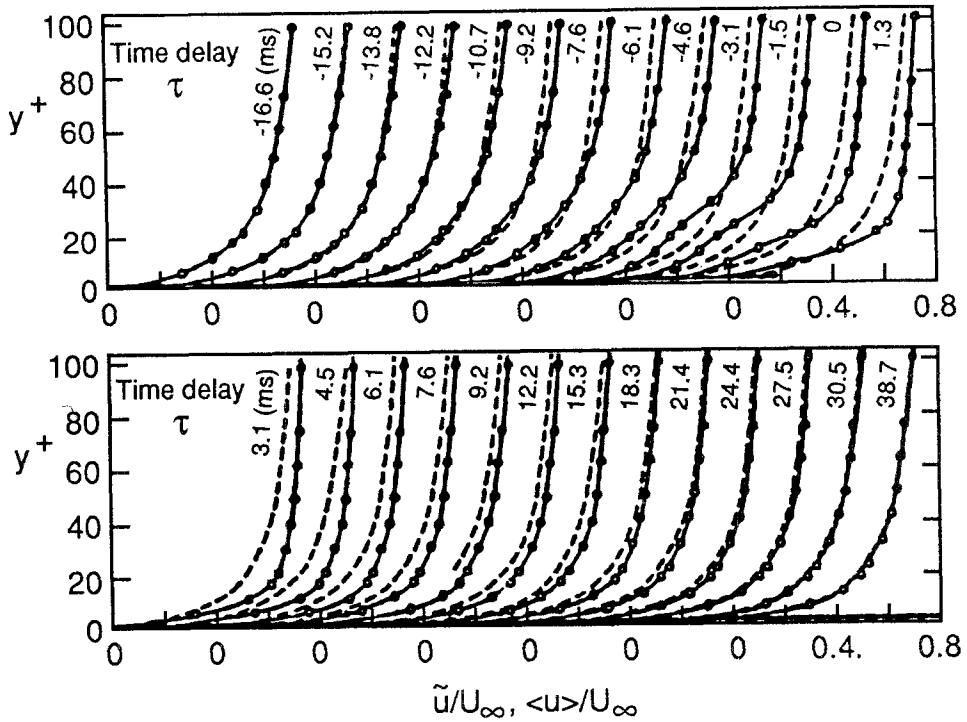

Fig. 7. Conditionally averaged velocity profiles before and after a burst, showing the influence on the local shear of the coherent structures (Blackwelder and Kaplan, 1976).

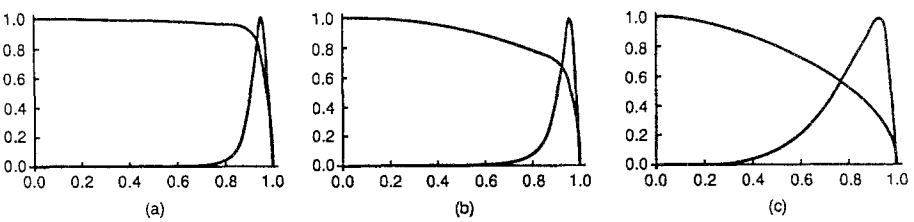

Fig. 8. The eigenfunctions generated by the anisotropic eddy viscosity model with various mean velocity profiles.

of the form $\langle u_i u_j \rangle v_{i,j}$. Consequently, we assume the perturbation stresses also to be a product:

$$r_{ij}(\mathbf{x}, t) = A(t)E(t)R_{ij}(\mathbf{x}). \tag{24}$$

Since we have used an eddy viscosity in obtaining the coherent forms we further assume that:

$$R_{ij}(\mathbf{x}) = -\nu_{ik}(\Psi_{j,k} + \Psi_{k,j}) \tag{25}$$

where $\nu_{11} = \nu_{22} = \nu_{33} = \nu_\tau$, $\nu_{12} = \nu_{21} = \beta_\tau$, $\nu_{13} = \nu_{23} = 0$. All that remains is to model the mean profile. For this we adopt the quasi-steady model used in Aubry

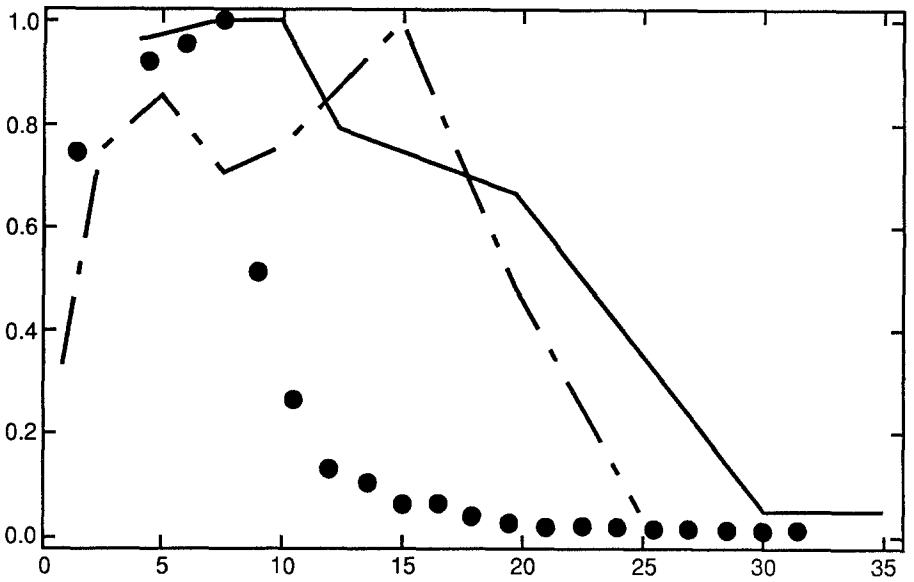

Fig. 9. •••• the POD eigenvalue spectrum; —·—·—· the eigenvalue spectrum generated by the anisotropic model without mean flow interaction; —— the eigenvalue spectrum generated with mean flow interaction.

et al. (1988). This allows the mean to respond to growing structures providing the necessary feed-back to the evolving modes. Using the friction velocity, u_τ, and the channel half height, a, the scaled equation for the mean gradient is:

$$\partial U(x_2,t)/\partial x_2 = \mathrm{Re}_\tau\{\langle u_1 u_2\rangle + \langle v_1 v_2\rangle - x_2\}. \tag{26}$$

The rate of dissipation of turbulent energy is given by a simple model adopted from second order closure schemes.

$$D\varepsilon/Dt = c_1(\varepsilon/k)\langle u_i u_k\rangle U_{i,k} - c_2\varepsilon^2/k + \text{Transport}. \tag{27}$$

Substituting these various models into the energy equations results in a set of three coupled ODEs for the temporal evolution of the energies and dissipation.

In order to evaluate the integrals appearing in these equations, we need to assume the spatial form of the averaged turbulence quantities B_{ij} and the dissipation $D(x_2)$. For this simple model we have assumed that while the intensity of the turbulence varies its spatial dependence remains unchanged. We use experimental data for fully developed turbulent channel flow to determine both B and D. The coherent structures are found by energy stability analysis, as described above.

5. Conclusions

The POD has played a central role in identifying coherent structures in experimental or computational data, and in constructing low-dimensional models of turbulent

flows, models which resolve only the coherent structures and their interaction, and parameterize the smaller scale, less organized turbulence. However, use of the POD raises a number of questions: is it the best way to identify the coherent structures? When we construct low-dimensional models, are we tied to Fourier decompositions in homogeneous directions, or can we use wavelets, and get away from periodic boundary conditions and periodic arrays of structures? Can we find cheaper ways to obtain the forms of the POD eigenfunctions, the coherent structures?

We have shown here that linear stochastic estimation, the other popular method for identification of coherent structures in experimental or computational data, is equivalent to the POD with the assumption that the coefficients in the POD are jointly Gaussian. For many purposes (so long as only second order quantities are being considered) this is a physically realistic assumption.

When we construct low-dimensional models using the POD, if there are homogeneous directions we have been accustomed to use Fourier decomposition. This is awkward physically, since the Fourier modes are not confined to a neighborhood while the disturbances to the real flow are. Here we have shown in connection with a one-dimensional equation that wavelets can be used instead with a negligible sacrifice in efficiency; and that simple assumptions regarding spatial interaction of the wavelets permits a relative simple model that reproduces the dynamics. This suggests that similar things are probably true of the Navier–Stokes equations, and that we will be able to construct low dimensional models for real flows, like the wall region of the boundary layer, using the more realistic wavelet representations, with reasonable truncations of the spatial interactions, thus freeing ourselves from periodic boundary conditions, and periodic arrays of coherent structures; we will thus be able to consider soliton coherent structures, which are much more realistic.

In order to construct these low-dimensional models, it is necessary to have at hand the POD eigenfunctions. Up to the present, this required extensive statistical documentation of the flow, either experimental or computational. Clearly, the flow with coherent structures represents a new attractor for the flow. We do not know how to analyze this new attractor to find the coherent structures. The coherent structures are extracting energy from the mean velocity profile, modifying it, and giving up energy to the small scale turbulence, also modifying it. We have suggested simple models for both modifications, and have shown that, with these adjustments, the form of the instability in its non-linear growth phase is essentially the same as the POD eigenfunctions, and the peak of the eigenvalue spectrum is in the same place. The flow whose instability we consider, of course, is the real flow with the coherent structures already present – we do not know how to remove them before we have them. Fortunately, it does not seem to make any difference. We may hope that, in poorly documented flows, we will have the same luck, and will be able to extract the eigenfunctions by a similar, relatively cheap, procedure.

References

Adrian, R. J., Conditional eddies in isotropic turbulence. *Physics of Fluids* 22(11) (1979) 2065–2070.

Adrian, R. J. and Moin, P., Stochastic estimation of organized turbulent structure: homogeneous shear flow. *J. Fluid Mech.* 190 (1988) 531–559.

Adrian, R. J., Moin, P., and Moser, R. D., Stochastic estimation of conditional eddies in turbulent channel flow. In: P. Moin, W.C. Reynolds and J. Kim (eds), *CTR, Proceedings of the Summer Program 1987*. NASA Ames Research Center/Stanford University (1987).

Aubry, N., Holmes, P., Lumley, J. L., and Stone, E., The dynamics of coherent structures in the wall region of a turbulent boundary layer. *J. Fluid Mech.* 192 (1988) 115–173.

Berkooz, G., *Turbulence, Coherent Structures and Low Dimensional Models*, Ph.D. Thesis, Cornell University (1991).

Berkooz, G., Elezgaray, J., and Holmes, P., Coherent structures in random media and wavelets. *Physica D* 61 (1993) 47–58.

Berkooz, G., Holmes, P., and Lumley, J. L., Intermittent dynamics in simple models of the turbulent wall layer. *J. Fluid Mech.* 230 (1991) 75–95.

Brereton, G. J. and Kodal, A., A frequency domain filtering technique for triple decomposition of unsteady turbulent flow. *J. Fluids Engineering* 114 (1992) 45–51.

Cantwell, B. J., Organized motions in turbulent flow. *Ann. Rev. Fluid Mech.* 13 (1981) 457–515.

Clavin, P., Dynamic behavior of premixed flame fronts in laminar and turbulent flows. *Prog. Energy Comb. Sci.* 11 (1985) 1–59.

Feller, W., *An Introduction to Probability Theory and Its Applications*. New York: John Wiley (1957).

Hyman, J. M. and Nicolaenko, B., The Kuramoto–Sivashinsky equation: a bridge between PDEs and dynamical systems. *Physica D* 18 (1986) 113–126.

Joseph, D. D., *Stability of Fluid Flow*. Berlin: Springer (1973).

Liu, J. T. C., Contributions to the understanding of large scale coherent structures in developing free turbulent shear flows. *Advances in Applied Mechanics* 26 (1988) 183–309.

Lumley, J. L., Some comments on the energy method. In: L. H. N. Lee and A H. Szewczyk (eds), *Developments in Mechanics 6*. Notre Dame, IN: N.D. Press (1971).

Moin, P. and Moser, R. D., Characteristic-eddy decomposition of turbulence in a channel. *J. Fluid Mech.* 200 (1989) 471–509.

Moin, P., Adrian, R. J., and Kim, J., Stochastic estimation of organized structures in turbulent channel flow. In: *6th Turbulence Shear Flow Symposium*, Toulouse, France (1987).

Poje, A., *An Energy Method Stability Model for Large Scale Structures in Turbulent Shear Flows*, Ph.D. Thesis, Ithaca, NY: Cornell (1993).

Poje, A. and Lumley, J. L., A model for large scale structures in turbulent shear flows. *J. Fluid Mechanics* (1994) (submitted).

Pomeau, Y., Pumir, A., and Pelce, P., Intrinsic stochasticity with many degrees of freedom. *J. Stat. Phys.* 37 (1984) 39–49.

Reynolds, W. C. and Hussain, A. K. M. F., The mechanics of an organized wave in turbulent shear flow. Part 3. Theoretical models and comparisons with experiment. *J. Fluid Mech.* 54 (1972) 263–287.

Reynolds, W. C. and Tiederman, W. G., Stability of turbulent channel flow with application to Malkus' theory. *J. Fluid Mech.* 27 (1967) 253–272.

Tennekes, H. and Lumley, J. L., *A First Course in Turbulence*. Cambridge, MA: The MIT Press (1972).

Zaleski, S., A stochastic model for the large scale dynamics for some fluctuating interfaces. *Physica D* 34 (1989) 427–438.